

MILITARY TECHNICAL COLLEGE
CAIRO - EGYPT7th INTERNATIONAL CONF. ON
AEROSPACE SCIENCES &
AVIATION TECHNOLOGY

Flow Pattern Solution for a Radial Blade Centrifugal Pump

W.A. Wahba^{*}, H.M. Abdalla^{**}, M.A. El-Senbawi^{***}

ABSTRACT

A theoretical investigation has been made to predict the flow pattern within a radial blade centrifugal pump. A mathematical model based on steady two-dimensional incompressible Navier-Stokes (N-S) equations has been developed. The real flow was modeled under these considerations. A computational-fluid-dynamic scheme was suggested using the primitive variables with artificial compressibility. The predictor-corrector method proposed by MacCormack was employed for its advantages of accuracy, less complexity, reasonable storage and convenient stability limit. A stability criterion was suggested and a fourth-order extrapolation smoothing term was used to limit the higher variations of the primitive variables. The use of this technique involved imaginary rows behind walls, and periodic boundaries at far upstream and downstream which adequately improved the convergence to the solution. Based on this model a computer program capable of predicting the flow pattern and pump characteristics inside the radial blade pump has been developed. The validity of the developed computer program, has been proven by comparing calculated and measured pump characteristic, which showed good agreement.

KEYWORDS

Flow Pattern - Radial Blade - Centrifugal Pump - Computational Fluid Dynamics.

1. INTRODUCTION

The investigation of the flow pattern inside the centrifugal pump is a basic object to select the pump suitable for a specific application. The flow pattern solution is a basic material to solve and predict the flow parameters inside the centrifugal pump. This work presents the

* Assistant, M.Sc., Department of Rockets, MTC, Cairo, Egypt.

** Assoc.Prof., Head of the Department of Rockets, MTC, Cairo, Egypt.

*** Ph.D., Department of Rockets, MTC, Cairo, Egypt.

development of steady two-dimensional, incompressible N-S equations in polar-coordinate system and their solution using primitive variables. The method was applied to a radial blade centrifugal pump. The difficult problem of calculating the flow pattern can be tackled after making a number of simplifying assumptions:

- The effect of turbulence is neglected and there is no separation of flow.
- The relative flow through the impeller passage is incompressible, and steady.
- The impeller is assumed rotating in an infinite field.
- The thickness of the impeller blades is neglected.
- The effect of the turn from the axial to radial direction is neglected.
- The velocity across the axial direction is constant and hence the flow is two-dimensional.

2. MAIN GOVERNING EQUATIONS

Consider the polar-coordinate system (r, θ) , where r denotes the radial direction and θ denotes the tangential direction. Consider the two-dimensional, incompressible N-S equations for a constant property flow without body forces or external heat addition. The continuity equation, written in the system relative to a blade row, is:

$$\frac{1}{\rho} \frac{\partial}{\partial r} (r u_r) + \frac{1}{\rho} \frac{\partial}{\partial \theta} (u_\theta) = 0 \quad (1)$$

where:

u_r, u_θ are relative flow velocity components in r and θ directions respectively.

ρ is the operating fluid density.

After the above assumptions, the momentum conservation law for a rotating blade is written as:

$$\frac{\partial}{\partial t} (u_r) + \frac{1}{r} \frac{\partial}{\partial r} (r u_r^2) + \frac{1}{r} \frac{\partial}{\partial \theta} (u_r u_\theta) - \frac{u_\theta^2}{r} - r \omega^2 - 2\omega u_\theta = -\frac{1}{\rho} \frac{\partial p}{\partial r} + \nu \left[\nabla^2 u_r - \frac{u_r}{r^2} - \frac{2}{r^2} \frac{\partial u_\theta}{\partial \theta} \right] \quad (2)$$

$$\frac{\partial}{\partial t} (u_\theta) + \frac{1}{r} \frac{\partial}{\partial r} (r u_r u_\theta) + \frac{1}{r} \frac{\partial}{\partial \theta} (u_\theta^2) + \frac{u_r u_\theta}{r} + 2\omega u_r = -\frac{1}{\rho r} \frac{\partial p}{\partial \theta} + \nu \left[\nabla^2 u_\theta - \frac{u_\theta}{r^2} + \frac{2}{r^2} \frac{\partial u_r}{\partial \theta} \right] \quad (3)$$

where:

p is static pressure.

ω is the angular velocity of the rotating blade.

ν is the kinematic viscosity.

$$\nabla^2 () = \frac{\partial^2}{\partial r^2} () + \frac{1}{r} \frac{\partial}{\partial r} () \frac{1}{r^2} \frac{\partial^2}{\partial \theta^2} () \quad (\text{for polar coordinates})$$

These equations are written in the so-called primitive-variable form where $p, u_r,$ and u_θ are the primitive-variables [1]. The computation of incompressible flows is not straight forward as in the case of computation of compressible flow. The most characteristic aspect of the computation of incompressible flow is the difficulty of extracting the pressure from the combined continuity and momentum equations. One common procedure is to define a Poisson equation or a specially formulated correction equation for the pressure. Application of compressible algorithms to the incompressible equations is accomplished by adding a time

derivative term to the continuity equation in a manner analogous to that originally suggested by Chorin [2].

The artificial density is related to the pressure by the artificial equation of state:

$$p = \delta \tilde{\rho} \quad (4)$$

where:

$\tilde{\rho}$ is the artificial density (variable).

δ is an artificial compressibility factor (constant).

Considering constant density ρ , the continuity equation (1) can be rewritten in the form:

$$-\frac{\partial}{\partial t}(\tilde{\rho}) = \rho \left[\frac{1}{r} \frac{\partial}{\partial r}(ru_r) + \frac{1}{r} \frac{\partial}{\partial \theta}(u_\theta) \right] \quad (5)$$

Substitution by Eq. 4 into Eq. 5 yields:

$$-\frac{\partial}{\partial t}(p) = \rho \delta \left[\frac{1}{r} \frac{\partial}{\partial r}(ru_r) + \frac{1}{r} \frac{\partial}{\partial \theta}(u_\theta) \right] \quad (6)$$

The following is a trial to investigate the artificial compressibility factor δ . An artificial equation of state implies the existence of an artificial sound speed (\tilde{a}^*) given by:

$$\tilde{a}^* = \sqrt{\frac{\partial p}{\partial \tilde{\rho}}} = \sqrt{\delta} \quad (7)$$

The maximum artificial Mach number (\tilde{M}_{\max}) based on this artificial sound speed is required to be less than unity.

$$\tilde{M} = \frac{\sqrt{(u_r^2 + u_\theta^2)_{\max}}}{\tilde{a}^*} = \frac{\sqrt{(u_r^2 + u_\theta^2)_{\max}}}{\sqrt{\delta}} \leq 1 \quad (8)$$

The following condition is obtained:

$$\delta \geq (u_r^2 + u_\theta^2)_{\max} \quad (9)$$

3. NUMERICAL ALGORITHM

3.1 Computational Grid

The computational domain is discretized into mesh points as shown in Fig. 1. The present scheme calculates the flow through one blade passage. The computational boundaries comprise the upstream inlet, the downstream exit, the pressure and suction side blade surfaces. The blade surfaces are extended along a surface of grid points in the upstream and downstream directions. These form permeable periodic boundaries. Logically, polar grid is used in the present method.

3.2 Finite Difference Scheme

There are two approaches to calculate incompressible N-S equations: implicit and explicit techniques. In this work the explicit one will be used. The most appropriate system of equations in differential form is the Reynolds averaged N-S equations in a rotating polar-coordinate system given by Lakshminarayana [3].

$$\frac{\partial Q}{\partial t} + \frac{1}{r} \frac{\partial(rE)}{\partial r} + \frac{1}{r} \frac{\partial F}{\partial \theta} = \frac{1}{r} S + \text{ViscousTerm} \quad (10)$$

where:

- Q** is the conservation variable.
- E, F** are the flux vectors.
- S** is the source term.

The viscous term will be discarded for its later use as central difference form in r and θ directions (Fig. 2). Equation (10) becomes:

$$\frac{\partial Q}{\partial t} = -\frac{1}{r} \frac{\partial(rE)}{\partial r} - \frac{1}{r} \frac{\partial F}{\partial \theta} + \frac{1}{r} S \quad (11)$$

Using Equations (2, 3, 6)

$$Q = \begin{bmatrix} P \\ u_r \\ u_\theta \end{bmatrix}, \quad E = \begin{bmatrix} \rho \delta u_r \\ u_r^2 + p/\rho \\ u_r u_\theta \end{bmatrix}, \quad F = \begin{bmatrix} \rho \delta u_\theta \\ u_r u_\theta \\ u_\theta^2 + p/\rho \end{bmatrix}, \quad \text{and} \quad S = \begin{bmatrix} 0 \\ u_\theta^2 + p/\rho + \omega^2 r^2 + 2\omega r u_\theta \\ -u_r u_\theta - 2\omega r u_r \end{bmatrix} \quad (12)$$

where the elements $[p/\rho]$ and $[p/\rho]$ in the flux vector **E** and source term **S** respectively are obtained from substituting $\left[-\frac{1}{\rho} \frac{\partial p}{\partial r}\right]$ in equation (2) with $\left[\frac{1}{r} \frac{p}{\rho} - \frac{1}{r} \frac{\partial}{\partial r}(r p/\rho)\right]$.

3.3 Predictor-Corrector Method

Predictor-Corrector method proposed by MacCormack [4] is a two-step procedure based on the Lax-Wendroff scheme, and is widely used for both internal and external flows. The method is second-order accurate in both time and space. It can be used for both steady and unsteady compressible flow, as well as viscous and inviscid flows. For the inviscid flow, in the procedure suggested by MacCormack, an iterative approach and intermediate value $\overline{Q}_{i,j}^{n+1}$ is obtained by a predictor step, and $Q_{i,j}^{n+1}$ is obtained by a corrector step, where n is the time step and $n+1$ is the next one. The predictor step written for the two dimensional (2-D) inviscid equations in polar (r, θ) system is given by:

$$\overline{Q}_{i,j}^{n+1} = Q_{i,j}^n - \frac{\Delta t}{\Delta r} [E_{i+1,j}^n - E_{i,j}^n] - \frac{\Delta t}{r_i \Delta \theta} [F_{i,j+1}^n - F_{i,j}^n] + \frac{S_{i,j} \Delta t}{r_i} \quad (13)$$

Here it should be emphasized that this step provides only an approximate value for $Q_{i,j}^{n+1}$, and this can be corrected or updated using the following corrector step:

$$Q_{i,j}^{n+1} = \frac{1}{2} \left\{ Q_{i,j}^n + \overline{Q}_{i,j}^{n+1} - \frac{\Delta t}{\Delta r} [\overline{E}_{i,j}^{n+1} - \overline{E}_{i-1,j}^{n+1}] - \frac{\Delta t}{r_i \Delta \theta} [\overline{F}_{i,j}^{n+1} - \overline{F}_{i,j-1}^{n+1}] + \frac{S_{i,j} \Delta t}{r_i} \right\} \quad (14)$$

where:

Δr is the element length in r direction.

$\Delta \theta$ is the element angle in θ direction.

The forward and backward differencing can be alternated between predictor and corrector steps as well as between the two spatial derivatives in a sequential fashion. The sequence is given in four time steps as shown in Table 1, in such a way to eliminate any bias due to the one-sided differencing. This procedure will be repeatedly carried out as required for the next four time steps.

Table 1. Differencing sequence for the MacCormack scheme*

Predictor		Corrector	
$\frac{\partial}{\partial r}$	$\frac{\partial}{\partial \theta}$	$\frac{\partial}{\partial r}$	$\frac{\partial}{\partial \theta}$
F	F	B	B
F	B	B	F
B	F	F	B
B	B	F	F

* (F = Forward, B = Backward)

3.4 Time Marching Procedure

The equations are solved using a time-marching procedure as is described in the following steps:

- 1) Specify initial values for u_r , u_θ , p at time $t = 0$.
- 2) Get stability condition which is used to converge the solution. In other words, calculate time steps Δt for all the grid points.
- 3) Solve the continuity equation and N-S equation at each interior grid point (predictor and corrector).
- 4) Perform the appropriate smoothing for the primitive variables to maintain stability in the numerical solution.
- 5) Find the primitive variables at the boundary using their values at the interior points.
- 6) Return to step 3 if the solution is not converged.

Practically, it was found that it is unnecessary to recalculate the stability condition (step 2) after performing each time step computation.

3.5 Smoothing Terms

For algorithms of the present type, it is often necessary to add smoothing terms in order to suppress high frequency oscillations. This can easily be accomplished by adding a fourth-order explicit dissipation term to the primitive variables in the two-directions of flow (r, θ) for interior points. The added term has the form:

$$-\varepsilon_e \left[(\Delta r)^4 \frac{\partial^4}{\partial r^4} (\mathbf{Q}) + (\Delta \theta)^4 \frac{\partial^4}{\partial \theta^4} (\mathbf{Q}) \right] \quad (15)$$

where ε_e is the explicit smoothing coefficient.

Since this is a fourth-order term it does not affect the formal accuracy of the algorithm. The negative sign is required in order to produce positive damping. The smoothing coefficient ε_e should be less than approximately 1/16 for stability [4]. A value of 0.05 is used in the present work. The fourth-derivative terms are evaluated using finite-difference approximations.

3.6 Stability Condition and Convergence Criteria

It is necessary to find a value of the time step Δt for which the stability of the solution could be maintained. For the inviscid and incompressible time marching method, a complete stability analysis is reported by Abdalla [5] who could express the maximum possible time step for the 2-D problem. Because of the complexity of N-S equations, it is not possible to obtain a closed form stability expression for the MacCormack scheme applied to the governing equations. Tannehill [4] used an empirical formula in case of one dimensional N-S equations. The expressions of Abdalla and Tannehill have been combined into one empirical formula, suitable for 2-D incompressible N-S equations, in the form [6]:

$$\Delta t = \left(\frac{2F_t}{\frac{|u_r|}{\Delta r} + \frac{|u_\theta|}{r\Delta\theta} + 4v \left(\frac{1}{(\Delta r)^2} + \frac{1}{(r\Delta\theta)^2} \right) + \sqrt{\left(\frac{u_r}{\Delta r} + \frac{u_\theta}{r\Delta\theta} \right)^2 + 4\delta \left(\frac{1}{(\Delta r)^2} + \frac{1}{(r\Delta\theta)^2} \right)}} \right) \quad (16)$$

where F_t is the time factor. It is found from experience that the time factor up to 0.9 can be used. In case of an unstable solution, the time factor is reduced by 0.1. Time steps are calculated based on the initial conditions and are not updated during the calculations. Thus, the time step varies as a function of grid spacing only. The iteration process is repeated until it converges. The computation is considered to be converged when the root mean square of the residual in the velocity component u_r drops below 10^{-5} .

$$\text{RMS} = \sqrt{\frac{\sum_{i=1}^{N_i-1} \sum_{j=1}^M |u_{r,i,j}^{n+1} - u_{r,i,j}^n|^2}{(N_i - 1)(M)}} \quad (17)$$

where:

- N_i is the total number of grid lines from upstream to downstream extensions in r direction.
- M is the number of grid lines from blade-to-blade in θ direction.

3.7 Upstream and Downstream Boundary Conditions

The prescription of the inflow and the outflow boundary conditions is one of the most important tasks. These surfaces should be located far upstream and far downstream, where the influence of the blade row under consideration is negligible. Hence, most investigators locate them usually at about one to one half-chord upstream and downstream. The far upstream and downstream boundaries are located about half-chord, and one-chord respectively as shown in Fig.1. On the upstream boundary the relative velocity components u_r and u_θ are specified. On the downstream boundary only the static pressure p is required. The other variables at both upstream and downstream boundaries are to be obtained by interpolation from the interior points.

3.8 Walls and their Extension Boundary Conditions

The wall points are considered as if they were interior points for the calculation of all the variables. This required to add a grid line before the pressure side and a grid line after the suction side as shown in Fig.1. The parameters at these lines were obtained by quadratic interpolation from the values at the wall and two interior points. This is numerically exactly the same as applying the conservation equations to a point on the half spacing near the wall and then extrapolating from this point to the boundary [5]. To simulate blade row conditions, it is essential to impose zero radial and tangential velocities in case of N-S equations. At the periodic boundary the variables were calculated as the interior points. In this case the periodicity condition could be used to obtain the variables which were located beyond the boundary. The results at corresponding points were then averaged after each time step.

3.9 Initial Conditions

The prescription of the flow for all grid points by relatively real values is one of the most important tasks. This initial guess can be completely arbitrary, where this procedure has no effect on the final solution, but it affects the number of iterations needed to converge the solution. Three zones of initial conditions are shown in Fig.1: imaginary upstream grid points (Z1), imaginary downstream grid points (Z3), and inside blade passage grid points (Z2). The data required for the solution are the major impeller dimensions, the flow rate, the fluid viscosity and density, and the impeller speed. The radial velocity is obtained from continuity. The tangential velocities in upstream and downstream are obtained from Euler's equation. Inside the blade passage, as the flow is considered radial, the tangential velocity is neglected. Assuming reasonable starting value for the downstream static pressure, Bernoulli constant at downstream is calculated. The initial values of the static pressure at all the grid points can be readily calculated.

3.10 Computer Code

The developed program is written in the C++ language (version 3.1 for Windows 3.x) with a total of about 800 statements. The execution file requires about 90 Kbytes of storage. Up to 52×23 grid points maximum, with a corresponding memory requirements of approximately 8 Mbytes, can be used. Time requirements per point per time step were about 7×10^{-4} seconds when a computer of type 486DX2-66MHz was used.

4. RESULTS AND DISCUSSION

The developed computer code was used to solve the case of an impeller with inner radius of 0.026 m, outer radius of 0.0625 m, number of blades is 6 and blade width is 0.01 m. The water was used as the working fluid, with flow rate ranging from 2 to 6 lit/s and pump speed of 1500 rpm. Different techniques were used to implement the boundary conditions to select the best technique from the point of view of convergence. Good improvement in the convergence of the solution was obtained with the use of imaginary rows behind walls and periodic boundaries at far upstream and downstream.

The convergence was predicted for flow rates of 0.002, 0.003, 0.004, 0.005 and 0.006 m³/s. Figure 3 shows the convergence histories for flow rate of 0.004 m³/s. Figure 3a shows the convergence of the RMS error in the radial velocity component. About 4000 iterations were required to obtain converged solution. The convergence of the outlet-to-inlet flow rate ratio is shown in Fig. 3b. It is clear that the ratio converges to a value very close to one. The convergence of the radial velocity component near the leading edge is shown in Fig. 3c. Figure 3d shows the convergence of the static pressure at the upstream boundary. To save computer memory and time single precision was used. As seen from the previous figures, a reasonable convergence was found for a number of iterations around 3000.

In order to check the validation of the presented code, it was applied to predict the performance of the given pump. The results were compared with the experimental data reported by Ahmmed [7], Fig.4. It was assumed that the pump characteristics depend mainly on the impeller characteristics. The head characteristic calculated by the code showed the correct trend. A close agreement with experimental data was demonstrated, in particular, around the nominal discharge Q_n . The static pressure distribution at the delivery and suction sides of the impeller is shown in Fig.5. In addition, distributions of relative velocities and pressure were calculated for the above flow rates. The results for a flow rate of 0.004 m³/s are shown in Fig.6. Figure 6a shows the radial relative velocity inside blade passage. The more developed flow downstream can be explained by larger flow area. Figure 6b shows the tangential relative velocity inside the blade passage. The difference of the tangential relative velocity inside the radial direction becomes more pronounced near the delivery side. The reverse flows are well indicated at this flow rate. Figure 6c shows the pressure contours inside blade passage. It is clear that for the same grid line, the pressure at the pressure side is higher than that at the suction one. The process of pump pressurization is obvious as the pressure increases in the downstream direction. The flow pattern at different flow rates is presented in Fig. 7. It could be seen that, at low flow rates the effect of rotation is dominant and hence a large vortex is formed, while at high flow rates the phenomenon is reversed.

5. CONCLUSION

A mathematical model based on the steady incompressible Navier-Stokes equations in two-dimensional polar-coordinate system has been developed. An explicit finite difference scheme has been used to solve the model. The pressure field solution was based on the artificial compressibility approach in which a time derivative pressure term was introduced into the conservation equation. Based on the above scheme, a computer code was developed and used to predict the flow pattern inside a radial blade centrifugal pump. The validity of the code was proven by comparing computational results with experimental data, which showed a close agreement. The code was used to calculate the head characteristic, the distributions of the

relative velocities and pressure for specified pump flow rates. The obtained impressive pictorial images of the flow might be highly required to interpret the many performance features of the pump.

REFERENCES

1. Hirsch C., and Warzee G., "A Finite-Element Method for Through Flow Calculations in Turbomachines", Transactions of the ASME, Journal of Fluids Engineering, pp. 403-410, 1976.
2. Chorin A.J., "A Numerical Method for Solving Incompressible Viscous Flow Problems", J. Comp. Phys., Vol. 2, pp. 12-26, 1967.
3. Lakshminarayana B., "An Assessment of Computational Fluid Dynamic Techniques in the Analysis and Design of Turbomachinery - The 1990 Freeman Scholar Lecture", Transactions of the ASME, Journal of Fluids Engineering, Vol. 113, pp. 315-352, 1991.
4. Anderson D.A., Tannehill J.C., and Pletcher R.H., Computational Fluid Mechanics and Heat Transfer, McGraw Hill Book Company, Second Edition, 1984.
5. Abdalla H., "A Theoretical and Experimental Investigation of the Regenerative Pump with Aerofoil Blades", Ph.D. Thesis, The Royal Military College of Science, 1981.
6. Wahba W.A., "Flow Pattern in A Centrifugal Pump used in Turbo-Pump Feed System", M.Sc. Thesis, Military Technical College, 1997.
7. Ahmmed E.A., "Study of Flow Field in a Radial Vaned Impeller of a Centrifugal Pump and its Effect on Pump Performance", M.Sc. Thesis, Military Technical College, 1995.

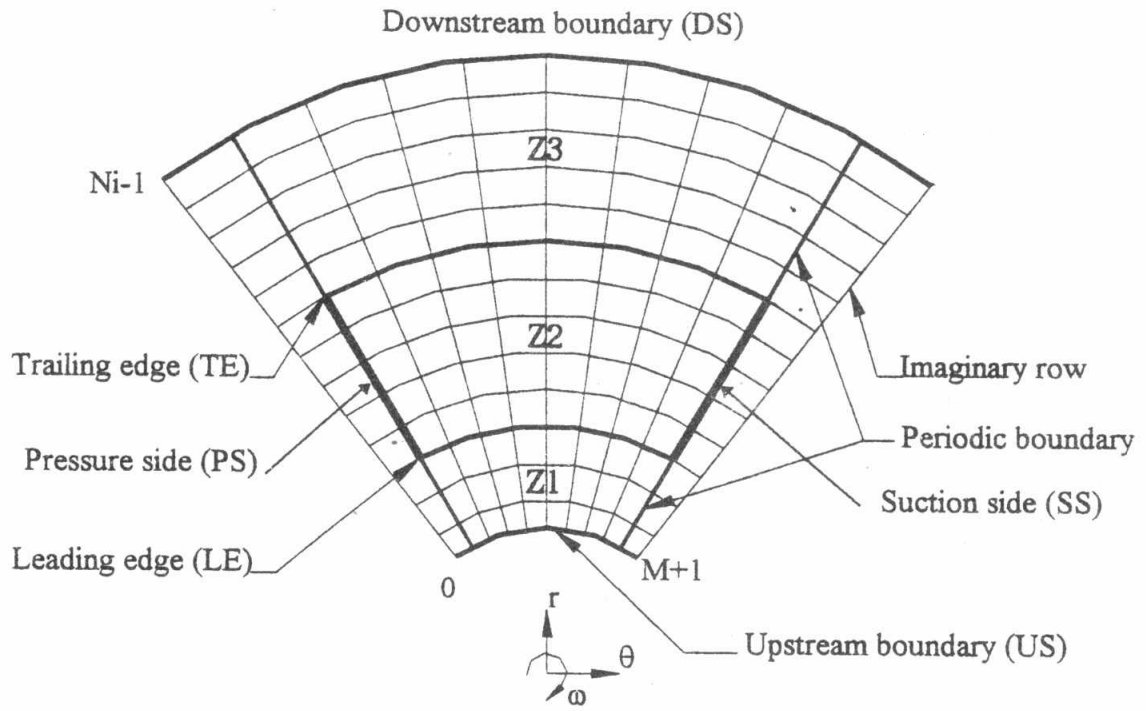


Fig. 1 Computational grid domain.

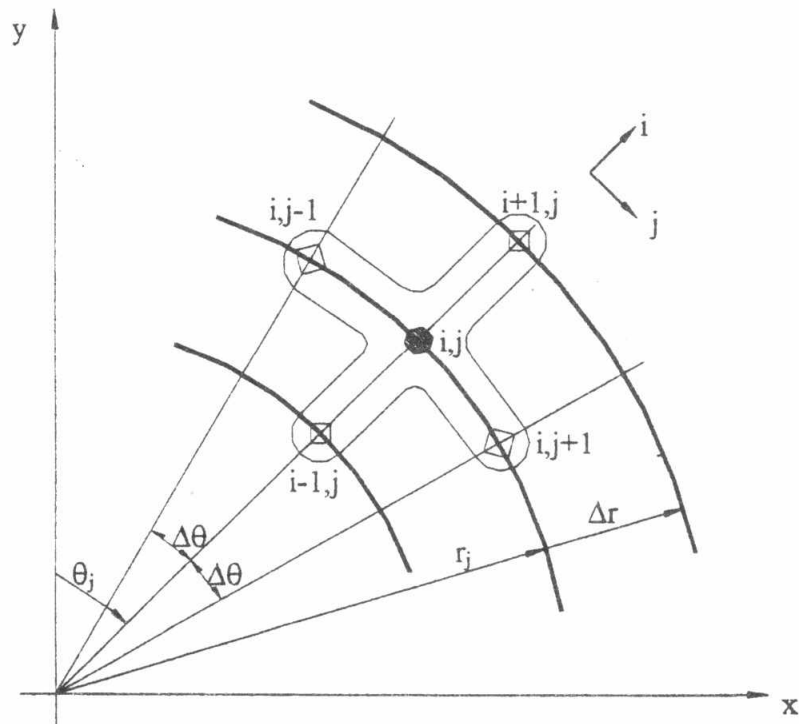
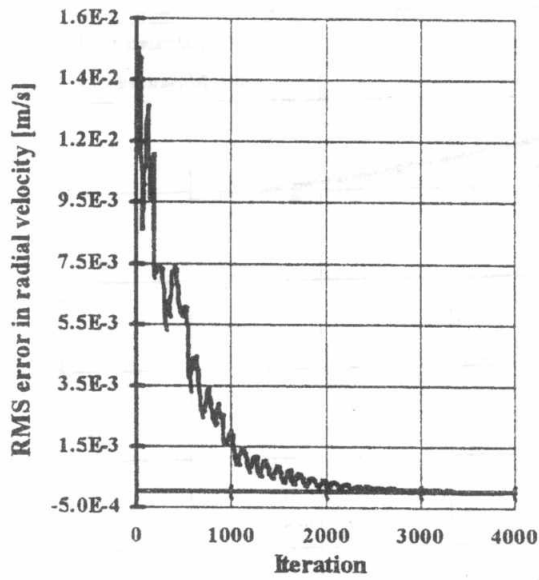
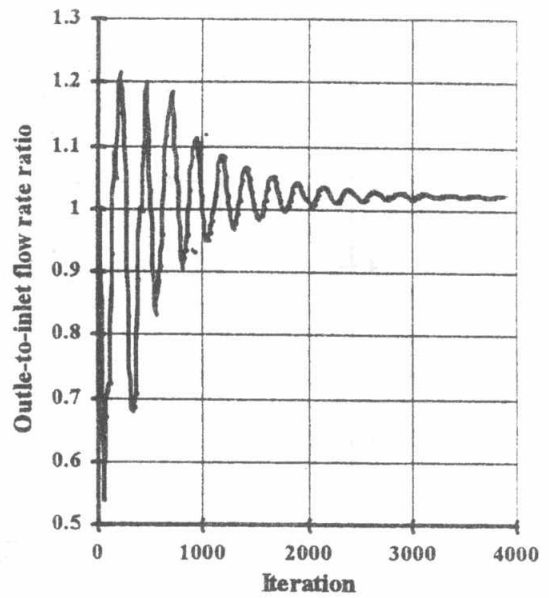


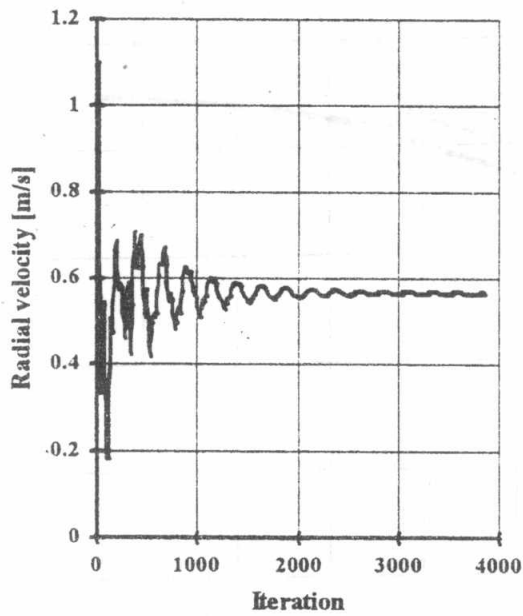
Fig. 2 The polar mesh.



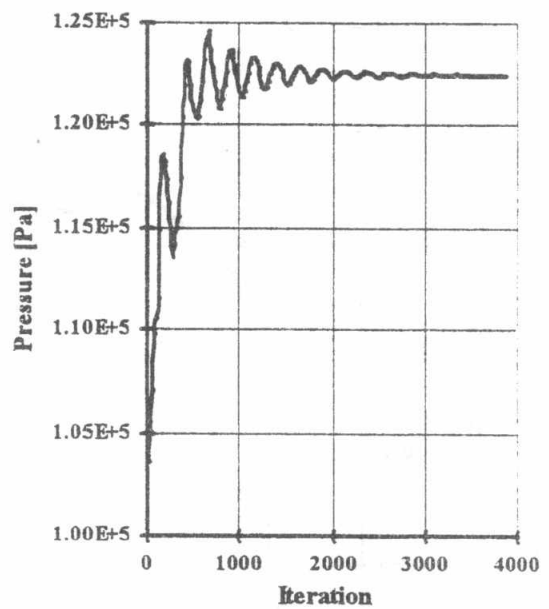
a. RMS error in radial velocity component.



b. Outlet-to-inlet flow rate ratio.



c. Radial velocity component near leading edge.



d. Static pressure at upstream boundary.

Fig.3 Convergence histories (Flow rate = 0.004 m³/s)

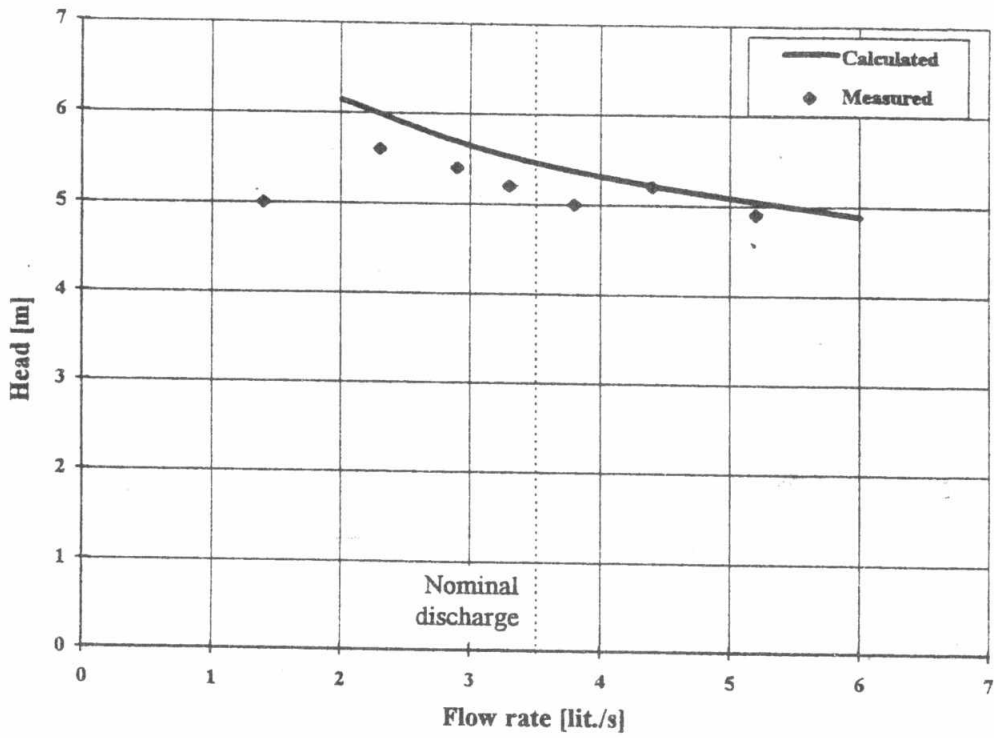


Fig.4 Comparison between the predicted pump performance and the measured values.

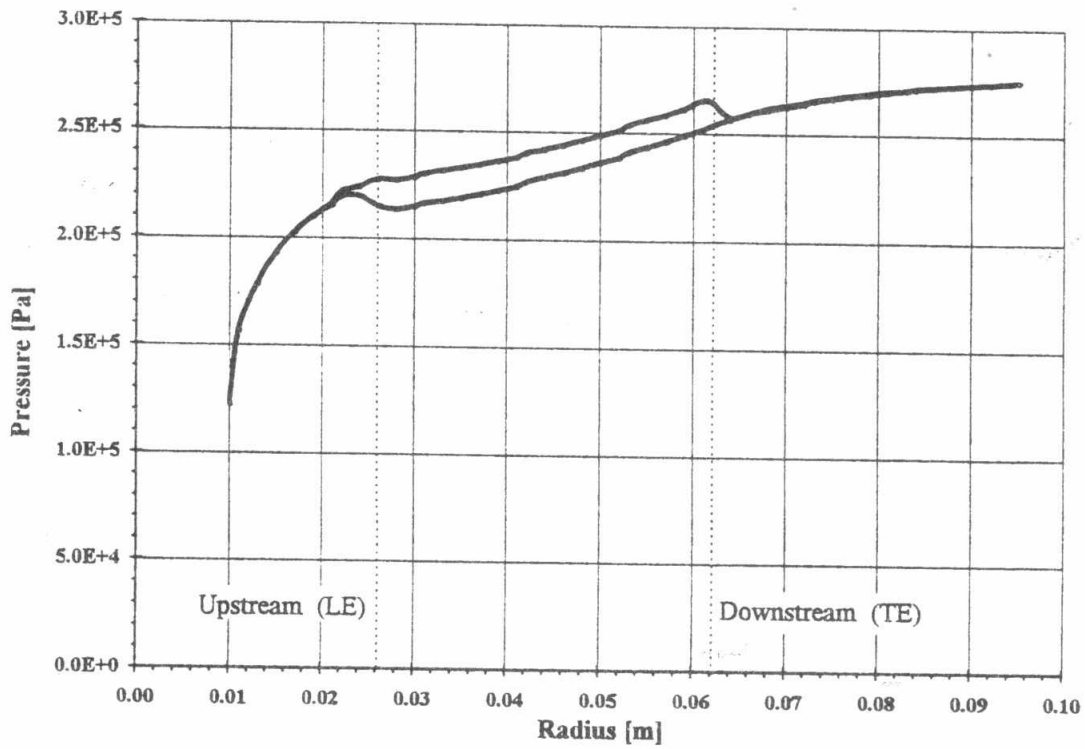
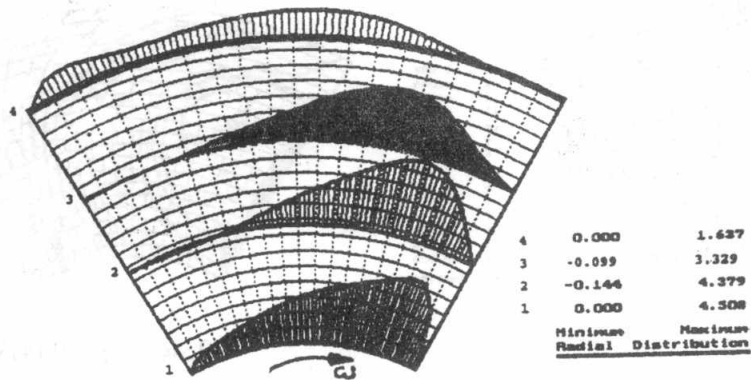
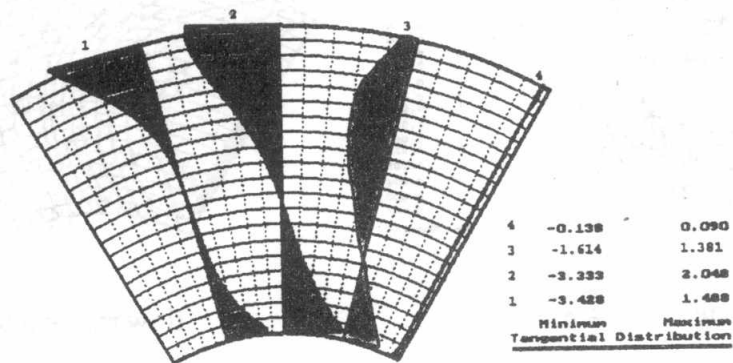


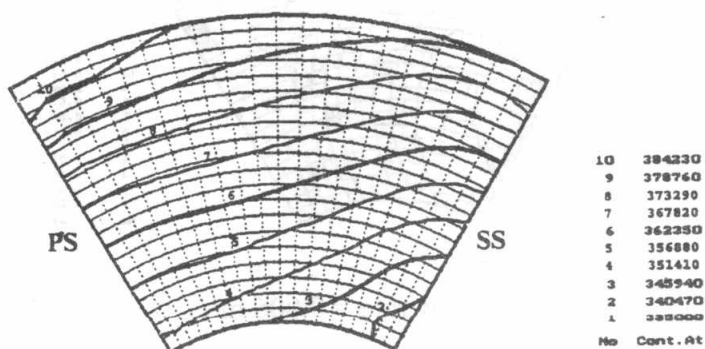
Fig.5 The static pressure distribution on the pressure and suction sides of the impeller.



a. Radial relative velocity.

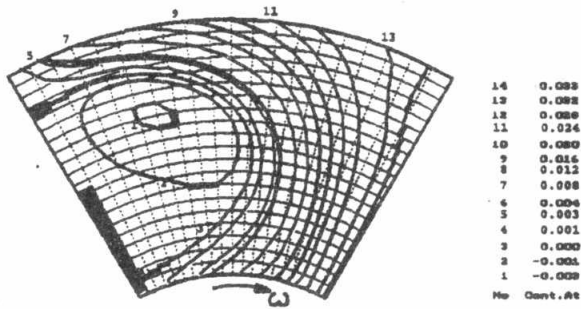


b. Tangential relative velocity.

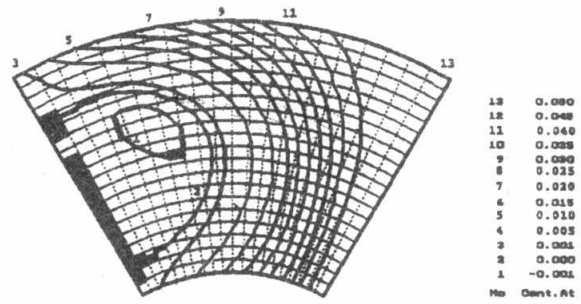


c. Pressure contours .

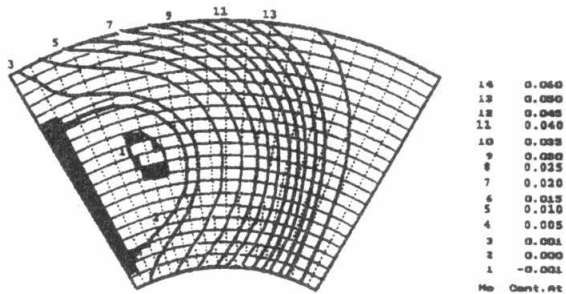
Fig.6 Distributions of relative velocities and pressure inside impeller blade passage (flow rate = 0.004 m³/s)



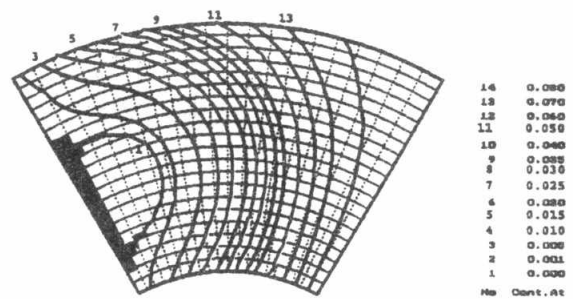
flow rate = 0.002 m³/s.



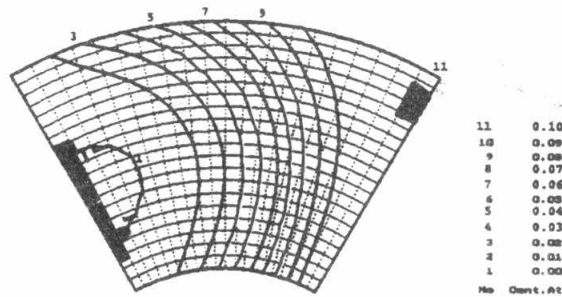
flow rate = 0.003 m³/s.



flow rate = 0.004 m³/s.



flow rate = 0.005 m³/s.



flow rate = 0.006 m³/s.

Fig.7 Flow pattern at different flow rates.